EUROPEAN RESPIRATORY *journal*

FLAGSHIP SCIENTIFIC JOURNAL OF ERS

Early View

Original article

Myeloperoxidase oxidation of methionine associates with early cystic fibrosis lung disease

Joshua D. Chandler, Camilla Margaroli, Hamed Horati, Matthew B. Kilgore, Mieke Veltman, H. Ken Liu, Alexander J. Taurone, Limin Peng, Lokesh Guglani, Karan Uppal, Young-Mi Go, Harm A.W.M. Tiddens, Bob J. Scholte, Rabindra Tirouvanziam, Dean P. Jones, Hettie M. Janssens

Please cite this article as: Chandler JD, Margaroli C, Horati H, *et al*. Myeloperoxidase oxidation of methionine associates with early cystic fibrosis lung disease. *Eur Respir J* 2018; in press (https://doi.org/10.1183/13993003.01118-2018).

MYELOPEROXIDASE OXIDATION OF METHIONINE ASSOCIATES WITH EARLY CYSTIC FIBROSIS LUNG DISEASE

Joshua D. Chandler[1,2,3], Camilla Margaroli[1,2], Hamed Horati[4], Matthew B. Kilgore[1,2], Mieke Veltman[4], H. Ken Liu[3], Alexander J. Taurone[5], Limin Peng[5], Lokesh Guglani[1,2], Karan Uppal[3], Young-Mi Go[3], Harm A.W.M. Tiddens[4], Bob J. Scholte[4], Rabindra Tirouvanziam[1,2*], Dean P. Jones[3*], Hettie M. Janssens[4*]

1. Center for CF and Airways Disease Research, Children's Healthcare of Atlanta, Atlanta, GA, USA

2. Division of Pulmonary, Allergy & Immunology, Cystic Fibrosis and Sleep Medicine, Department of Pediatrics, Emory University, Atlanta, GA, USA

3. Division of Pulmonary, Allergy and Critical Care Medicine, Department of Medicine, Emory University, Atlanta, GA, USA

4. Department of Pediatric Pulmonology, Erasmus Medical Center / Sophia Children's Hospital, Rotterdam, The Netherlands

5. Department of Biostatistics, Emory University School of Public Health, Atlanta, GA, USA

*Co-senior authors

Corresponding author:

Rabindra Tirouvanziam, PhD

Emory Children's Center, 2015 Uppergate Dr NE, Rm 344, Atlanta, GA 30322, USA

Ph: +1 404 712 7684; Email: tirouvanziam@emory.edu

Funding and author contributions:

Supported by NHLBI F32 HL132493 (JDC); Emory Children's CF & Airways Disease Research Center Startup Fund (JDC, MK); CFF P30 MCCART15R0 (CM); NHLBI R01 HL126603, Common Fund for Metabolomics Supplement HL126603-02S1 and Dutch Cystic Fibrosis Foundation [NCFS] grant HIT-CF 1 and 2 (HH, MV, BJS, HMJ, AP, AT, LP, RT); ERARE INSTINCT (MV, BJS), and P30 ES019776, S10 OD018006, and R01 ES023485 (HKL, KU, YMG, DPJ).

Experimental conception and design: RT, HMJ, BJS, JDC. Performed experiments: JDC, HH, CM, MBK, MV. Interpreted results and provided critical support: JDC, HH, CM, MBK, HKL, BJS, HAWMT, AJT, LP, LG, KU, YMG, HMJ, DPJ, RT. Prepared manuscript: JDC. Reviewed or edited and approved manuscript: All authors.

Running Title: Methionine oxidation in CF lung disease.

Manuscript body word count: 3306

"Take home" summary statement

Identifying molecules associated with early cystic fibrosis lung disease may lead to new means of limiting progression. We found that airway fluid methionine sulfoxide produced by myeloperoxidase associates with lung disease in CF patients aged 1-3 years.

Short sentence

Methionine oxidation is associated with airway myeloperoxidase activity and structural damage in infants with CF.

This article has an online data supplement which is accessible from this issue's table of content online at www.atsjournals.org.

Abstract

Rationale

Cystic fibrosis (CF) lung disease progressively worsens from infancy to adulthood. Disease-driven changes in early CF airway fluid metabolites may identify therapeutic targets to curb progression.

Methods

CF patients aged 12-38 months (n=24; 3/24 later denoted as CF screen positive, inconclusive diagnosis) received chest computed tomography scans, scored by the PRAGMA-CF method to quantify total lung damage (PRAGMA-%Dis) and components such as bronchiectasis. Small molecules in bronchoalveolar lavage fluid (BALF) were measured with high-resolution, accurate-mass metabolomics. Myeloperoxidase was quantified by ELISA and activity assays.

Results

Increased PRAGMA-%Dis was driven by bronchiectasis and correlated with airway neutrophils. PRAGMA-%Dis correlated with 104 metabolomic features ($p<0.05$, $q<0.25$). The most significant annotated feature was methionine sulfoxide, a product of methionine oxidation by myeloperoxidase-derived oxidants. We confirmed the identity of methionine sulfoxide in BALF and used reference calibration to confirm correlation with PRAGMA-%Dis (Spearman's $\boldsymbol{\rho}=0.582$, $p=0.0029$), extending to bronchiectasis (PRAGMA-%Bx; $\boldsymbol{\rho}=0.698$, $p=1.5\times10^{-4}$), airway neutrophils ($\boldsymbol{\rho}=0.569$, $p=0.0046$) and BALF myeloperoxidase ($\boldsymbol{\rho}=0.803$, $p=3.9\times10^{-6}$).

Conclusions

BALF methionine sulfoxide associates with structural lung damage, airway neutrophils and myeloperoxidase in early CF. Further studies are needed to establish whether methionine oxidation directly contributes to early CF lung disease and explore potential therapeutic targets indicated by these findings.

Keywords: Innate immunity, Oxidative stress, Orbitrap, CFSPID, Hypochlorous acid

Introduction

Cystic fibrosis (CF) is a multi-organ disease caused by genetic mutations affecting expression, stability, regulation and/or function of the cystic fibrosis transmembrane conductance regulator (CFTR) anion channel protein. CF is characterized by progressive bronchiectasis resulting in respiratory failure, the primary cause of mortality (1). During childhood, CF airways exhibit neutrophilic inflammation, infections and impaired mucociliary clearance (2). Inflammation may be key to lung disease development due to its early onset, before routine detection of pathogens. Indeed, presence of neutrophil elastase (NE) in airway fluid was the strongest predictor of development of persistent bronchiectasis in a study of young children with CF (3). Neutrophil release of primary granules, which contain NE, myeloperoxidase (MPO) and other proteins capable of injuring airway mucosa, is a plausible mechanism of CF airway disease pathogenesis (4). Recognizing the earliest onset of inflammation in CF and underlying mechanisms is key to limiting disease progression.

Airway lining fluid, chiefly regulated by epithelia, could play major roles in promoting CF airway inflammation (5, 6). CFTR regulates airway fluid composition and volume directly and through interaction with other proteins, such as the epithelial sodium channel (ENaC) (1). When CFTR function is insufficient, airway fluid may change in ways that promote disease, either providing direct pro-inflammatory cues or injuring airway cells (7). Incoming neutrophils, via intense metabolic and effector activities, may further alter CF airway fluid. Due to the complexity of human airway physiology, unbiased methodologies such as untargeted metabolomics may serve to identify unanticipated biochemical changes driving pathogenesis.

Sensitive chest computed tomography (CT) techniques have been developed to detect early lung disease in CF patients. One such method, the Perth-Rotterdam Annotated Grid Morphometric Analysis for CF (PRAGMA-CF), can quantify bronchiectasis, mucus plugging, air trapping, and other airway abnormalities in CF patients younger than 6 years (8). Lung imaging may be combined with bronchoalveolar lavage (BAL) to survey airway fluid and cells to find associations with structural lung disease. For example, protein-bound glutathione from BAL fluid (BALF) was previously associated with higher risk of developing bronchiectasis (9). Untargeted analyses have identified dozens of candidate metabolite biomarkers for the detection of CF lung disease (10). Transition from biomarkers to mechanisms of pathology may lead to new therapeutic strategies to treat early lung disease in CF.

Here we hypothesized that metabolites in early CF BALF linked to disease progression should correlate with PRAGMA-CF. We applied high-resolution, accurate-mass mass spectrometry (HRMS)-based metabolomics to identify correlations in CF children who underwent prospective BAL and chest CT. We confirmed the identity of the most significant identified metabolite (methionine sulfoxide) and quantified MPO, an enzyme from neutrophils capable of generating it through production of strong oxidants.

Materials and Methods

Study design

The study was performed as part of the Inflammatory Markers in Broncho-Alveolar Lavage Fluid for Lung Disease in Infants with Cystic Fibrosis (I-BALL) study (clinicaltrial.gov identifier, NCT02907788). It is a translational, exploratory and observational study of infants with CF identified by newborn screening in which BALF, peripheral blood, chest CT and clinical follow-up data are prospectively collected. The IRB of the Erasmus MC approved the study (IRB protocol NL49725.078.14), and all parents signed informed consent.

Sample collection

Bronchoscopy and CT were scheduled prospectively following enrollment and took place within 3 consecutive days on average. Patients fasted overnight prior to the BAL procedure, taking place under general anesthesia. Twenty-four right middle lobe BAL samples were collected from CF patients aged 12-38 months. One ml/kg body weight sterile saline was instilled and recovered three times and research samples pooled from second and third aliquots were placed on ice for no more than 2 h before BALF was isolated by centrifugation at 330 *g* and 4 ˚C for 5 min, then stored at -80 ˚C. The first BAL aliquot was used for clinical pathology, including bacterial culture and cell counts. Free-breathing chest CT scan were acquired without anesthesia using Siemens SOMATOM® Force ultra-fast scanner. PRAGMA-CF was used for quantitative scoring of percentages of bronchiectasis (PRAGMA-%Bx) and total lung disease (PRAGMA-%Dis) (8). CT scans were interpreted by a single observer blinded to other study

information at the time of scoring. %Dis was a composite of PRAGMA-%Bx, mucus plugging and bronchial wall thickening. Additional demographics and findings are in **Table 1**.

Metabolomics

Metabolites were extracted from BALF by 1:2 mixture with acetonitrile (ACN) plus internal standards, carried out on ice for 30 minutes followed by vortexing and centrifugation at 16,000 *g* and 4 ˚C for 10 min. Supernatant was maintained on an autosampler held at 4 ˚C and analyzed via Q Exactive High Field (Thermo) hybrid mass spectrometer. Intensities of detected mass-to-charge (*m/z*) features were extracted using apLCMS 6.3.3 (11), evaluated for data quality using xMSanalyzer 2.0.8 (12), and pre-filtered as detailed in the **Online Supplement**. Significant features were annotated using METLIN (13). Standard Reference Material (SRM) 1950 (National Institute of Standards and Technology) was analyzed in parallel to the BALF samples as a quality control and reference standard.

MPO assay

Abundance and activity of MPO were quantified in an assay adapted from Chapman *et al*. (14). Briefly, MPO is immunocaptured, and its abundance and activity are measured by ELISA and Amplex Red oxidation, respectively. Assay lower limits of quantification of 1.0 ng/ml (Amplex Red) and 0.13 ng/ml (ELISA) were established from three independent assays.

Statistics

Metabolomics data analysis, including $\log_2$ transformation, quantile normalization and Pearson's correlation with p-value calculation and false discovery rate-adjusted q-value calculation, was performed using an in-house R package (https://github.com/kuppal2/xmsPANDA). We selected q<0.25 for multiple comparisons adjustment of metabolomics results due to the convolution inherent to electrospray ionization mass spectra (multiple signals can be observed per compound). Additional analysis was performed using MetaboAnalyst (15) and ggplot2 (16). MPO assays were calibrated by SoftMax Pro v. 7.0.3 (Molecular Devices). Prism 7 (GraphPad) was used to calculate Spearman correlations and Mann-Whitney U test, and to generate figures.

Additional methods are located in the Supplementary Information document accompanying this manuscript.

Results

Patient characteristics and CT determination of lung disease

Patient characteristics are shown in **Table 1**. Fifty percent of patients were homozygous for F508del, and all but one carried at least one copy of the allele. Three genotyped with an R117H-7T allele and sweat chloride <60 mmol/l were re-designated as CF screened positive, inconclusive diagnosis (CFSPID; highlighted in red in barplot and scatterplot figures; range of sweat chloride, 24-55 mmol/l) (17). Over 90% of patients were on antibiotics at the time of the procedure, and less than half of patients were positive for pathogenic organisms by BAL culture.

PRAGMA-CF analysis was conducted on CT scans acquired at 1, 2 or 3 years of age. PRAGMA-CF analysis identified the presence of bronchiectasis in most of the patients (PRAGMA-%Bx; 0 to 3.74%), while the composite score (PRAGMA-%Dis) ranged from 0.82 to 7.47%. Clinical variables, such as gender, F508del homozygosity, and positive BAL culture, did not significantly influence PRAGMA-%Dis, or we did not consider them because data distributions were unevenly skewed (e.g., pancreatic insufficiency).

Metabolomics

A list of 11,188 *m/*z-by-retention time features was initially recovered from BALF samples (**Supplementary File 1**), and a working feature table of 1,798 was produced by applying thresholds for intensity, technical precision and missing values. One sample was determined to have an aberrant number of missing values and removed from the study (**Supplementary Figure 1A-B**). Data were then $\log_2$-transformed and quantile

normalized prior to testing (**Supplementary Figure 1C**). Ultimately, 190 features were significant at $p<0.05$, and 104 of these passed $q<0.25$ multiple comparisons-adjusted threshold (results in **Supplementary File 2**). Significant features were annotated in METLIN (13), and we assigned 30 annotations matching a total of 22 unique metabolites (**Figure 1** and **Table 2**). In cases of multiple ions belonging to the same metabolite, data for the ion of highest average intensity is shown.

The most significant annotated feature matched to methionine sulfoxide (MetO; **Table 2**). Several metabolites corresponded to pathways of arginine metabolism (including arginine, citrulline, ornithine, diacetylspermine) or to glycerophospholipids and lysolipids. Others included lithocholic acid, trigonelline and several other amino acids. Most were positively associated with PRAGMA-%Dis, but three – phosphatidylcholine (PC) 42:6, phosphatidylethanolamine acyl/ether (PE ae) 32:0, and lithocholic acid – were inversely associated. Twelve unidentified features ranging from 675-861 *m/z* and co-eluting at 330 sec showed strong positive correlations with PRAGMA-%Dis (**Supplementary File 2**; $r > 0.6$, $p \leq 0.001$ for all), but these produced no reasonable database matches and were not further assessed.

Identification and reference calibration of methionine sulfoxide

We sought to confirm the accurate mass annotation of MetO (**Figure 1** and **Table 2**; representative trace in **Supplementary Figure 2A**). We synthesized isotopically enriched $^{13}C_5$,^{15}N-L-MetO and spiked this into pooled CF BALF and SRM 1950 to identify MetO by stable isotope co-elution and MS/MS. Naturally occurring and isotopically enriched MetO gave rise to the same five fragments with appropriate mass

shifts in the isotopically enriched reagent (**Supplementary Figures 2B-C**), providing confirmation of the 2D structure of MetO in both BALF and SRM 1950 (**Supplementary Figure 2D**).

We calibrated MetO and methionine in SRM 1950 to enable reference calibration of the BALF samples and calculate the percentage of MetO relative to the sum of MetO and Met (% OxMet). SRM 1950 was calibrated at 20.68 µM methionine (93% of the NIST-certified reference value, 22.3 µM) and 1.22 µM MetO, corresponding to 5.6% OxMet. MetO was then reference calibrated in BALF and ranged from 24 to 1,031 nM (mean 174±240 nM), while % OxMet ranged from 3.8 to 62.7% (18.8±14.8%). After calibration, MetO remained significantly correlated with PRAGMA-%Dis using non-parametric Spearman's correlation (**Figure 2A**).

Quantification of MPO in CF BALF

MetO is produced by the reaction of Met with myeloperoxidase (MPO)-derived oxidants hypochlorous (HOCl) and hypobromous acid (HOBr) (18). MPO was detected in BALF and exhibited the same immunoreactivity as in blood neutrophils (**Supplementary Figure 3**). We determined the catalytic activity and protein abundance of MPO in CF BALF to evaluate its potential relationships with PRAGMA-%Dis and MetO. MPO ranged from 0.0087 to 4.5 µg/ml in CF BALF (mean 0.90±1.17 µg/ml), except for one CFSPID sample in which none was detected. MPO distribution was non-normal and was similar when normalized to protein (**Supplementary Figure 4A**). BALF MPO was active in an Amplex Red-based peroxidase assay and none of the samples exhibited low activity percentage relative to ELISA results (**Supplementary Figure 4B-**

C). BALF MPO correlated strongly with PRAGMA-%Dis (**Figure 2B**), as well as MetO (**Figure 2C**).

Relationships of MetO and MPO with bronchiectasis and neutrophils

We sought to understand the specific contributions of bronchiectasis (PRAGMA-%Bx) and the percentage of airway neutrophils to MetO, % OxMet and MPO. We performed pairwise Spearman correlations for these variables (**Table 3**). For each of the variables, including airway neutrophils, PRAGMA-%Bx resulted in a stronger correlation than PRAGMA-%Dis. The strongest observed correlation between two independent variables was that of % OxMet and MPO.

Robustness of key correlations

To ensure robustness of key correlations, we analyzed a subset of patients by excluding three CFSPID-designated samples and five others for whom clinical complications prevented the completion of BAL and CT procedures within 28 consecutive days. After removing the total eight samples, MetO remained significantly correlated with PRAGMA-%Bx (**Supplementary Figure 5B**) and MPO (**Supplementary Figure 5C**), but the significant association with PRAGMA-%Dis was lost (**Supplementary Figure 5A**). Because the strength of the subset correlation ($\boldsymbol{\rho}$=0.4353) was comparable to the original ($\boldsymbol{\rho}$=0.5817), decreased power probably explains the lack of significance. MPO remained significantly correlated with PRAGMA-%Dis (**Supplementary Figure 4D**) and PRAGMA-%Bx (**Supplementary Figure 4E**).

Global correlations

To compare the global correlations of MetO, MPO and PRAGMA-CF to clinical variables, we prepared a Spearman's correlation matrix (**Figure 3**). We considered BAL immune cell percentages, BALF total protein, patient age, sweat chloride, and the number of antibiotic (Abx) courses. The three strongest correlations with PRAGMA-%Dis were MPO, MetO, and % BAL macrophages ($\boldsymbol{\rho}$=-0.5824, p=0.0036) and with PRAGMA-%Bx were MPO, MetO and % BAL neutrophils. BAL % PMNs and % macrophages exhibited a strong inverse relationship ($\boldsymbol{\rho}$=-0.9683, p=3.9×10^{-14}). Age and BALF protein also had positive correlations with PRAGMA-%Dis and PRAGMA-%Bx. BAL % eosinophils, BAL % lymphocytes, sweat chloride and the number of antibiotic courses in the past 12 months were not correlated with other variables.

Discussion

Taken together, our results are consistent with the early emergence of neutrophilic influx, granule exocytosis and oxidizing activity of secreted MPO early in CF pathology, particularly bronchiectasis (scheme in **Figure 4**). The contribution of neutrophilic inflammation to CF lung disease is well recognized, yet exact mechanisms of pathogenesis are not fully understood. Interventions directly targeting inflammation in CF are currently limited to high-dose ibuprofen, and no FDA-approved therapies specifically target airway neutrophils (19). Such an intervention might be most effective and have the longest-lasting benefits if administered in earliest stages of CF (20). It is not yet known how CFTR modulators will influence inflammation in the lungs, and these drugs are not yet available for young children.

The present study demonstrates the potential importance of methionine oxidation by MPO in early CF lung disease. Airway MetO and % OxMet strongly correlated with MPO, indicating that MPO is responsible for the MetO detected. Biomarker studies have indicated that MPO does generate HOCl and HOBr in CF airways (21). Distinct oxidants with diverse reactivity profiles are generated in the airways that may serve to help or harm the host, with HOCl and HOBr associated with lasting molecular damage (22). These oxidants have exceptional reduction potentials and rapidly oxidize methionine (18, 23), while weaker oxidants and those that are kinetically restrained, such as hypothiocyanous acid and hydrogen peroxide (respectively), react much more slowly with methionine, so that their contributions to its oxidation *in vivo* may effectively be nil (24, 25). The strong correlation observed for MPO and % OxMet in this cohort support the notion that MPO generates significant HOCl and HOBr in CF airways at a young

age. Importantly, MPO may do this regardless of the source of H_2O_2, which is generated *in vivo* from multiple physiological processes (26). Although phagocyte NADPH oxidase 2 is a likely contributor to neutrophil-derived hydrogen peroxide (via superoxide), other sources of H_2O_2 should not be ruled out.

While the influence of MPO is well recognized in CF airway pathophysiology (9, 21), this study is, to the best of our knowledge, the first time that MetO and % OxMet have been identified as correlates of bronchiectasis and airway neutrophils in young children with CF, which we discovered using an unbiased metabolomics approach. Of note, untargeted mass spectral data may incur multiple comparison penalties that are ultimately too conservative, as multiple interdependent spectra can arise from individual chemicals in the samples (27), resulting in a higher likelihood of type II error (28). Recognizing this, we used a moderate multiple comparisons threshold of $q<0.25$ for untargeted mass spectral data. However, we note that multiple metabolites including MetO would have surpassed more stringent thresholds. Although our data suggest that methionine is one of the most sensitive airway metabolites to the advancement of neutrophilia and bronchiectasis in early CF, additional studies are needed to validate the importance of methionine oxidation in early CF. In addition to these findings, our study confirms the relationship of % OxMet and MPO in CF BALF previously identified by Dickerhof and co-workers (9).

To maximize clinical utility, airway MetO and % OxMet measurements should be extended in future studies to include less invasive samples, such as exhaled breath condensate (EBC), sputum and tracheal aspirates. While we anticipate that sputum and tracheal aspirates will be sufficiently concentrated to perform robust metabolomics

research, methodological innovations to improve sensitivity for dilute EBC samples are a necessity. Fortunately, mass spectrometry has already been demonstrated to be amenable to CF EBC metabolite detection (29). Standardized collection in accordance with best clinical practice is also crucial, particularly in early stage pediatric studies where reproducible sample acquisition can be challenging.

Correlations of MetO and % OxMet with bronchiectasis are consistent with previously hypothesized redox dysregulation and oxidative stress in CF. Much attention has been placed on decreased abundance and accelerated oxidation of glutathione in CF airways (9, 30, 31). By contrast, we found that cystine (the homodimeric disulfide of cysteine) was positively correlated with PRAGMA-%Dis. Because the samples were not treated to preserve thiols, the result may be indicative of the total cysteine and cystine pool rather than the oxidized form alone. This indicates that glutathione and cysteine likely support divergent redox signaling pathways in airways, much like other physiological compartments (32). We did not detect the irreversibly oxidized glutathione sulfonamide in the current study, which may be due to methodological differences and/or reflect its low abundance, possibly limited by its stringent reaction (3 mol of HOCl or HOBr react with 1 mol glutathione) (33).

The association of MetO and early CF bronchiectasis could result from multiple pathophysiological processes. Excessive and sustained neutrophil transmigration is associated with progressive airway damage (34), and is a necessary precursor to the accumulation of luminal MPO required for efficient methionine oxidation by HOCl/HOBr. However, neutrophils secrete several other potentially damaging factors, and MetO could represent multiple pathways of damage by proxy. For example, MPO release is

generally concomitant with that of neutrophil elastase (4). However, additional experiments are needed to establish the relationship of these enzymes in early CF. In particular, future studies will assess whether MPO-dependent MetO production may be readily measurable in infants with CF while elastase activity may not, due to airway antiprotease shield that counterbalances elastase effectively early on in the disease process (3).

In contrast to MetO, which associated more strongly with PRAGMA-%Bx than PRAGMA-%Dis, methionine was the opposite: associated more strongly with PRAGMA-%Dis than with PRAGMA-%Bx (however, neither association was as strong as those of MetO; data not shown). This reversal may reflect association of methionine with different disease processes not directly related to MPO activity, such as bulk movement of metabolites into the airway lumen with neutrophils, or the methionine salvage pathway. The methionine salvage pathway, in which methionine and adenine are recovered from byproducts of polyamine biosynthesis, has been implicated in worse lung function in CF by genome-wide association and transcriptomic studies indicating potential roles for *AMD1*, *MTAP* and *APIP* (35-37). Airway methionine oxidation might promote increased expression of this pathway, and such potential for pathological cross-talk should be considered in future studies. Additional studies are also needed to determine the extent to which the steady-state redox potential of methionine is actively maintained in airways, including individual fates of the MetO stereoisomers, methionine-*S*-sulfoxide and methionine-*R*-sulfoxide. These are reduced back to methionine by distinct enzymes (38), although mammals do not encode an efficient free methionine-(R)-sulfoxide reductase (39).

Inflammation in CF may be present from an extremely early age, provoked by inherent epithelial defects (7). A recent study in children under 18 years of age showed a decreased rate of annual lung function decline and increased long-term survival in high dose ibuprofen-exposed patients (40). The effects of high-dose ibuprofen may include inhibition of neutrophil oxidative burst (41), which would in turn limit production of HOCl and HOBr from MPO. Many compounds have been investigated as candidate MPO inhibitors, including 2-thioxanthines and acetaminophen (42, 43). Such drugs may find utility in limiting early CF lung disease, but this requires further testing. Other interventions directly targeting key reactive species such as HOCl may also have potential to limit airway disease caused by hypohalous acids (44-47). Strategies to limit oxidative imbalance in CF should take the species of oxidants generated and their respective roles into account, as oxidants serve diverse and critical roles in host defense and redox signaling processes (22, 26).

We included three patients with R117H-7T mutations, designated CFSPID after initial enrollment via newborn screening, in the study. Interestingly one of the patients showed significant inflammation, heightened MetO and increased PRAGMA-CF scores on chest CT, despite having a mutation which is considered as non-CF causing. Therefore, PRAGMA-CF and BAL studies that are useful in identifying lung disease processes in CF appear to have some applicability to CFSPID as well. Future studies may identify environmental and genetic factors that promote neutrophilic lung disease in otherwise healthy CFSPID and/or in well-controlled CF.

In conclusion, we present data that demonstrate the importance of methionine oxidation via MPO in early CF airway disease. MetO, % OxMet and MPO strongly

correlated with PRAGMA-%Dis and PRAGMA-%Bx, sensitive measures of early lung disease and bronchiectasis. Our initial discovery was made through an unbiased metabolomics method and confirmed using targeted analyses. MetO and MPO should be further studied in pathological mechanisms underlying early onset CF airway disease, which may lead to novel biomarkers and targets for therapy.

Acknowledgments

We thank patients and families for consenting to participate in this study. We acknowledge research coordinators E. Nieuwhof, E. van der Wiel and B. Manai for their support in recruiting patients. We thank Dr. Pijnenburg, Dr. de Jongste, Dr. Duijts, Dr. Kloosterman and Dr. de Kleer for performing bronchoscopies. We thank M. Kemner for her guidance with PRAGMA-CF scoring. We thank Dr. Nina Dickerhof for insightful technical discussions about the MPO assay method.

References

1. Elborn JS. Cystic fibrosis. *Lancet* 2016;388:2519–2531.

2. Stoltz DA, Meyerholz DK, Welsh MJ. Origins of Cystic Fibrosis Lung Disease. *N Engl J Med* 2015;372:351–362.

3. Sly PD, Gangell CL, Chen L, Ware RS, Ranganathan S, Mott LS, Murray CP, Stick SM, AREST CF Investigators. Risk factors for bronchiectasis in children with cystic fibrosis. *N Engl J Med* 2013;368:1963–1970.

4. Margaroli C, Tirouvanziam R. Neutrophil plasticity enables the development of pathological microenvironments: implications for cystic fibrosis airway disease. *Molecular and Cellular Pediatrics* 2016;3:38.

5. Hartl D, Gaggar A, Bruscia E, Hector A, Marcos V, Jung A, Greene C, McElvaney G, Mall M, Döring G. Innate immunity in cystic fibrosis lung disease. *J Cyst Fibros* 2012;11:363–382.

6. Forrest OA, Ingersoll SA, Preininger MK, Laval J, Limoli DH, Brown MR, Lee FE, Bedi B, Sadikot RT, Goldberg JB, Tangpricha V, Gaggar A, Tirouvanziam R. Frontline Science: Pathological conditioning of human neutrophils recruited to the airway milieu in cystic fibrosis. *J Leukoc Biol* 2018;16:45.

7. Montgomery ST, Mall MA, Kicic A, Stick SM. Hypoxia and sterile inflammation in cystic fibrosis airways: mechanisms and potential therapies. *Eur Respir J* 2017;49:1600903–13.

8. Rosenow T, Oudraad MCJ, Murray CP, Turkovic L, Kuo W, de Bruijne M, Ranganathan SC, Tiddens HAWM, Stick SM, Australian Respiratory Early Surveillance Team for Cystic Fibrosis (AREST CF). PRAGMA-CF. A Quantitative Structural Lung

Disease Computed Tomography Outcome in Young Children with Cystic Fibrosis. *Am J Respir Crit Care Med* 2015;191:1158–1165.

9. Dickerhof N, Pearson JF, Hoskin TS, Berry LJ, Turner R, Sly PD, Kettle AJ, AREST CF. Oxidative stress in early cystic fibrosis lung disease is exacerbated by airway glutathione deficiency. *Free Radic Biol Med* 2017;113:236–243.

10. Esther CR, Turkovic L, Rosenow T, Muhlebach MS, Boucher RC, Ranganathan S, Stick SM, AREST CF. Metabolomic biomarkers predictive of early structural lung disease in cystic fibrosis. *Eur Respir J* 2016;48:1612–1621.

11. Yu T, Park Y, Johnson JM, Jones DP. apLCMS--adaptive processing of high-resolution LC/MS data. *Bioinformatics* 2009;25:1930–1936.

12. Uppal K, Soltow QA, Strobel FH, Pittard WS, Gernert KM, Yu T, Jones DP. xMSanalyzer: automated pipeline for improved feature detection and downstream analysis of large-scale, non-targeted metabolomics data. *BMC Bioinformatics* 2013;14:1–1.

13. Guijas C, Montenegro-Burke JR, Domingo-Almenara X, Palermo A, Warth B, Hermann G, Koellensperger G, Huan T, Uritboonthai W, Aisporna AE, Wolan DW, Spilker ME, Benton HP, Siuzdak G. METLIN: A Technology Platform for Identifying Knowns and Unknowns. *Anal Chem* 2018;doi:10.1021/acs.analchem.7b04424.

14. Chapman ALP, Mocatta TJ, Shiva S, Seidel A, Chen B, Khalilova I, Paumann-Page ME, Jameson GNL, Winterbourn CC, Kettle AJ. Ceruloplasmin is an endogenous inhibitor of myeloperoxidase. *J Biol Chem* 2013;288:6465–6477.

15. Xia J, Sinelnikov IV, Han B, Wishart DS. MetaboAnalyst 3.0—making metabolomics more meaningful. *Nucleic Acids Res* 2015;43:W251–W257.

16. Wickham H. *ggplot2: Elegant Graphics for Data Analysis*, 1st ed. New York, NY: Springer New York; 2009. doi:10.1007/978-0-387-98141-3.

17. Salinas DB, Sosnay PR, Azen C, Young S, Raraigh KS, Keens TG, Kharrazi M. Benign and Deleterious Cystic Fibrosis Transmembrane Conductance Regulator Mutations Identified by Sequencing in Positive Cystic Fibrosis Newborn Screen Children from California. *PLoS ONE* 2016;11:e0155624.

18. Pattison DI, Davies MJ. Absolute rate constants for the reaction of hypochlorous acid with protein side chains and peptide bonds. *Chem Res Toxicol* 2001;14:1453–1464.

19. Taylor-Cousar JL, Kessel Von KA, Young R, Nichols DP. Potential of anti-inflammatory treatment for cystic fibrosis lung disease. *J Inflamm Res* 2010;3:61–74.

20. Grasemann H, Ratjen F. Early lung disease in cystic fibrosis. *Lancet Respir Med* 2013;1:148–157.

21. Thomson E, Brennan S, Senthilmohan R, Gangell CL, Chapman ALP, Sly PD, Kettle AJ. Identifying peroxidases and their oxidants in the early pathology of cystic fibrosis. *Free Radic Biol Med* 2010;49:1354–1360.

22. Chandler JD, Day BJ. Biochemical mechanisms and therapeutic potential of pseudohalide thiocyanate in human health. *Free Radic Res* 2015;49:695–710.

23. Arnhold J, Monzani E, Furtmüller PG, Zederbauer M, Casella L, Obinger C. Kinetics and Thermodynamics of Halide and Nitrite Oxidation by Mammalian Heme Peroxidases. *Eur J Inorg Chem* 2006;2006:3801–3811.

24. Skaff O, Pattison DI, Davies MJ. Hypothiocyanous acid reactivity with low-molecular-mass and protein thiols: absolute rate constants and assessment of biological relevance. *Biochem J* 2009;422:111–117.

25. Winterbourn CC. The biological chemistry of hydrogen peroxide. *Methods Enzymol* 2013;528:3–25.

26. Go Y-M, Chandler JD, Jones DP. The cysteine proteome. *Free Radic Biol Med* 2015;84:227–245.

27. Dunn WB, Erban A, Weber RJM, Creek DJ, Brown M, Breitling R, Hankemeier T, Goodacre R, Neumann S, Kopka J, Viant MR. Mass appeal: metabolite identification in mass spectrometry-focused untargeted metabolomics. *Metabolomics* 2013;9:44–66.

28. Wang B, Shi Z, Weber GF, Kennedy MA. Introduction of a new critical p value correction method for statistical significance analysis of metabonomics data. *Anal Bioanal Chem* 2013;405:8419–8429.

29. Zang X, Monge ME, McCarty NA, Stecenko AA, Fernández FM. Feasibility of Early Detection of Cystic Fibrosis Acute Pulmonary Exacerbations by Exhaled Breath Condensate Metabolomics: A Pilot Study. *J Proteome Res* 2017;16:550–558.

30. Kettle AJ, Turner R, Gangell CL, Harwood DT, Khalilova IS, Chapman AL, Winterbourn CC, Sly PD, on behalf of AREST CF. Oxidation contributes to low glutathione in the airways of children with cystic fibrosis. *Eur Respir J* 2014;erj01702–2013.doi:10.1183/09031936.00170213.

31. Day BJ, van Heeckeren AM, Min E, Velsor LW. Role for Cystic Fibrosis Transmembrane Conductance Regulator Protein in a Glutathione Response to Bronchopulmonary. *Infect Immun* 2004;72:2045–2051.

32. Kemp M, Go Y-M, Jones DP. Nonequilibrium thermodynamics of thiol/disulfide redox systems: A perspective on redox systems biology. *Free Radic Biol Med* 2008;44:921–937.

33. Harwood DT, Kettle AJ, Winterbourn CC. Production of glutathione sulfonamide and dehydroglutathione from GSH by myeloperoxidase-derived oxidants and detection using a novel LC–MS/MS method. *Biochem J* 2006;399:161.

34. Fuschillo S, De Felice A, Balzano G. Mucosal inflammation in idiopathic bronchiectasis: cellular and molecular mechanisms. *Eur Respir J* 2008;31:396–406.

35. Polineni D, Dang H, Gallins PJ, Jones LC, Pace RG, Stonebraker JR, Commander LA, Krenicky JE, Zhou Y-H, Corvol H, Cutting GR, Drumm ML, Strug LJ, Boyle MP, Durie PR, Chmiel JF, Zou F, Wright FA, O'Neal WK, Knowles MR. Airway Mucosal Host Defense Is Key to Genomic Regulation of Cystic Fibrosis Lung Disease Severity. *Am J Respir Crit Care Med* 2018;197:79–93.

36. Corvol H, Blackman SM, lle P-YBE, Gallins PJ, Pace RG, Stonebraker JR, Accurso FJ, Clement A, Collaco JM, Dang H, Dang AT, Franca A, Gong J, Guillot L, Keenan K, Li W, Lin F, Patrone MV, Raraigh KS, Sun L, Zhou Y-H, Neal WKOR, Sontag MK, Levy H, Durie PR, Rommens JM, Drumm ML, Wright FA, Strug LJ, *et al.* Genome-wide association meta-analysis identifies five modifier loci of lung disease severity in cystic fibrosis. *Nature Commun* 2015;6:1–8.

37. Dang H, Gallins PJ, Pace RG, Guo X-L, Stonebraker JR, Corvol H, Cutting GR, Drumm ML, Strug LJ, Knowles MR, O'Neal WK. Novel variation at chr11p13 associated with cystic fibrosis lung disease severity. *Hum Genome Var* 2016;3:16020–5.

38. Lee BC, Lee HM, Kim S, Avanesov AS, Lee A, Chun B-H, Vorbruggen G, Gladyshev VN. Expression of the methionine sulfoxide reductase lost during evolution extends Drosophila lifespan in a methionine-dependent manner. *Sci Rep* 2018;8:1010.

39. Lee BC, Le DT, Gladyshev VN. Mammals reduce methionine-S-sulfoxide with MsrA and are unable to reduce methionine-R-sulfoxide, and this function can be restored with a yeast reductase. *J Biol Chem* 2008;283:28361–28369.

40. Konstan MW, VanDevanter DR, Sawicki GS, Pasta DJ, Foreman AJ, Neiman EA, Morgan WJ. Association of High-Dose Ibuprofen Use, Lung Function Decline, and Long-Term Survival in Children with Cystic Fibrosis. *Annals ATS* 2018;doi:10.1513/AnnalsATS.201706-486OC.

41. Nielsen VG, Webster RO. Inhibition of human polymorphonuclear leukocyte functions by ibuprofen. *Immunopharmacology* 1987;13:61–71.

42. Koelsch M, Mallak R, Graham GG, Kajer T, Milligan MK, Nguyen LQ, Newsham DW, Keh JS, Kettle AJ, Scott KF, Ziegler JB, Pattison DI, Fu S, Hawkins CL, Rees MD, Davies MJ. Acetaminophen (paracetamol) inhibits myeloperoxidase-catalyzed oxidant production and biological damage at therapeutically achievable concentrations. *Biochem Pharmacol* 2010;79:1156–1164.

43. Tidén A-K, Sjögren T, Svensson M, Bernlind A, Senthilmohan R, Auchère F, Norman H, Markgren P-O, Gustavsson S, Schmidt S, Lundquist S, Forbes LV, Magon NJ, Paton LN, Jameson GNL, Eriksson H, Kettle AJ. 2-thioxanthines are mechanism-based inactivators of myeloperoxidase that block oxidative stress during inflammation. *J Biol Chem* 2011;286:37578–37589.

44. Casaril AM, Ignasiak MT, Chuang CY, Vieira B, Padilha NB, Carroll L, Lenardão EJ, Savegnago L, Davies MJ. Selenium-containing indolyl compounds: Kinetics of reaction with inflammation-associated oxidants and protective effect against oxidation of extracellular matrix proteins. *Free Radic Biol Med* 2017;113:395–405.

45. Conrad C, Lymp J, Thompson V, Dunn C, Davies Z, Chatfield B, Nichols D, Clancy J, Vender R, Egan ME, Quittell L, Michelson P, Antony V, Spahr J, Rubenstein RC, Moss RB, Herzenberg LA, Goss CH, Tirouvanziam R. Long-term treatment with oral N-acetylcysteine: affects lung function but not sputum inflammation in cystic fibrosis subjects. A phase II randomized placebo-controlled trial. *J Cyst Fibros* 2015;14:219–227.

46. Griese M, Kappler M, Rietschel E, Hartl D, Hector A. Inhalation Treatment with Glutathione in Patients with Cystic Fibrosis. A Randomized Clinical Trial. *Am J Respir Crit Care Med* 2013;188:83–89.

47. Chandler JD, Min E, Huang J, McElroy CS, Dickerhof N, Mocatta T, Fletcher AA, Evans CM, Liang L, Patel M, Kettle AJ, Nichols DP, Day BJ. Antiinflammatory and Antimicrobial Effects of Thiocyanate in a Cystic Fibrosis Mouse Model. *Am J Respir Cell Mol Biol* 2015;53:193–205.

TABLES

Table 1. Patient characteristics and clinical findings

Children[a] (n)	24
Age (months)	31 ± 11
Female:Male (n)	16:8
F508del homozygous (%)	50.0
Sweat chloride (mmol/l)	92±28
Pancreatic insufficiency (%)	87.5
Using antibiotics at BAL (%)	91.2
Past antibiotic courses[b]	2.9 ± 1.9
Secondhand smoke (%)	29.2
BAL neutrophils[c] (%)	27.7 ± 18.9
BAL macrophages[c] (%)	64.6 ± 19.7
BAL lymphocytes[c] (%)	7.2 ± 4.7
BAL eosinophils[c] (%)	0.5 ± 0.8
Positive BAL culture (%)[c]	39.1
Positive for *S. aureus* (%)[c]	26.1
Positive for *P. aeruginosa* (%)[c]	4.3

Data are mean ± SD or a percentage. [a]All subjects received prospective BAL and CT procedures. [b]Number of antibiotic courses received (oral and/or i.v., including prophylaxis) 12 months prior to the prospective visit (n=18). [c]n=23.

Table 2. Metabolites correlated with PRAGMA-%Dis in untargeted analysis.

m/z	*Time (sec)*	*Metabolite*	*Adduct*	*Error (ppm)*	r	*p-value*	*q-value*
166.0533	281	Methionine sulfoxide	[M+H]	0	0.648	5.59E-5	0.0273
862.6339	137	PC 42:6	[M+H]	2	-0.357	9.89E-5	0.0273
524.3711	270	LysoPC 18:0	[M+H]	0	0.669	3.57E-4	0.0407
287.2442	320	Diacetylspermine	[M+H]	0	0.318	6.36E-4	0.0425
522.3556	270	LysoPC 18:1	[M+H]	0	0.599	2.69E-3	0.1272
175.1190	305	Arginine	[M+H]	0	0.254	2.78E-3	0.1272
496.3397	274	LysoPC 16:0	[M+H]	0	0.598	2.86E-3	0.1272
133.0972	308	Ornithine	[M+H]	0	0.304	2.98E-3	0.1277
482.3240	196	LysoPE 18:0	[M+H]	0	0.579	3.70E-3	0.1428
466.3288	192	LysoPE O-18:1	[M+H]	0	0.640	4.80E-3	0.1586
147.1128	311	Lysine	[M+H]	0	0.197	6.72E-3	0.1920
176.1030	257	Citrulline	[M+H]	0	0.307	8.68E-3	0.2061
112.0869	303	Histamine	[M+H]	0	0.284	9.54E-3	0.2152
808.5817	215	PC 36:2	[M+Na]	1	0.161	0.0127	0.2314
415.2607	222	Lithocholic acid	[M+K]	0	-0.193	0.0141	0.2314
526.2913	192	LysoPE 22:6	[M+H]	2	0.310	0.0159	0.2431
660.5332	157	PE ae 32:0	[M+H-H2O]	0	-0.049	0.0183	0.2456
772.6232	218	PC ae 36:2	[M+H]	2	0.678	0.0186	0.2456
205.0971	182	Tryptophan	[M+H]	0	0.309	0.0198	0.2467
703.5729	247	SM 34:1	[M+H]	2	0.150	0.0205	0.2467

241.0311	306	Cystine	[M+H]	0	0.420	0.0207	0.2467
138.0550	267	Trigonelline	[M+H]	0	0.153	0.0221	0.2467

Metabolites $p<0.05$, $q<0.25$ are shown following deconvolution to remove redundant features that correspond to the same chemical. In such cases, the *m/z* feature with the highest mean intensity was selected.

Table 3. Pairwise correlations of variables associated with lung disease.

	PRAGMA-%Bx	PMNs (%)	MetO (nM)	%OxMet	MPO (µg/ml)
PRAGMA-%Dis	n = 24 $\boldsymbol{\rho}$ = 0.726 p = 5.8 x 10^{-5}	n = 23 $\boldsymbol{\rho}$ = 0.502 p = 0.0146	n = 24 $\boldsymbol{\rho}$ = 0.582 p = 0.0029	n = 24 $\boldsymbol{\rho}$ = 0.437 p = 0.0286	n = 23 $\boldsymbol{\rho}$ = 0.706 p = 1.7 x 10^{-4}
PRAGMA-%Bx		n = 23 $\boldsymbol{\rho}$ = 0.6742 p = 4.2 x 10^{-4}	n = 24 $\boldsymbol{\rho}$ = 0.698 p = 1.5 x10^{-4}	n = 24 $\boldsymbol{\rho}$ = 0.665 p = 3.9 x 10^{-4}	n = 23 $\boldsymbol{\rho}$ = 0.752 p = 3.5 x 10^{-5}
PMNs (%)			n = 23 $\boldsymbol{\rho}$ = 0.569 p = 0.0046	n = 23 $\boldsymbol{\rho}$ = 0.594 p = 0.0028	n = 22 $\boldsymbol{\rho}$ = 0.656 p = 0.0092
MetO (nM)				n = 24 $\boldsymbol{\rho}$ = 0.860 p = 7.2 x 10^{-8}	n = 23 $\boldsymbol{\rho}$ = 0.803 p = 3.9 x 10^{-6}
%OxMet					n = 23 $\boldsymbol{\rho}$ = 0.837 p = 6.4 x 10^{-7}

Pairwise Spearman correlation results are shown for the listed variables. Note that the variable pairs of PRAGMA-%Dis and PRAGMA-%Bx and that of MetO and %OxMet are not independent (PRAGMA-%Bx contributes directly to PRAGMA-%Dis, and MetO contributes directly to %OxMet).

FIGURE LEGENDS

Figure 1. Accurate mass metabolite annotations of *m/z* features significantly associated with PRAMGA-%Dis. Intensities of *m/z*-by-retention time features measured from CF BALF by HRMS were $\log_2$-transformed, quantile-normalized and correlated with PRAGMA-%Dis using a linear model. Of 104 significant ($p<0.05$, $q<0.25$) features, 28 were annotated to accurate mass matches using METLIN. These corresponded to 22 unique metabolites after deconvolution of co-eluting compounds (see also Table 2; and the complete dataset given in Supplementary File 2). The *m/z* feature with highest average intensity for each of the 22 metabolites was plotted on a heatmap, autoscaled to Z-scores and coded blue-(most negative)-to-red (most positive). Missing values are represented as gray. Columns were sorted from left-to-right by ascending PRAGMA-%Dis and rows were hierarchically clustered by metabolite intensities. Accurate mass metabolite matches are indicated to the right of the heatmap. PRAGMA-%Dis values corresponding to each patient are shown by a barplot above the heatmap. Bar color corresponds to disease state (white = CF, red = CFSPID). Bar fill corresponds to BAL microbe culture (no fill = no history of positive pathogen culture, diagonal lines = negative for pathogens at time of BAL, but a prior BAL was positive, and hatched = positive pathogen culture at time of BAL).

Figure 2. Correlations of structural lung disease, methionine oxidation and myeloperoxidase in early CF. Spearman correlations were analyzed for pairwise combinations of PRAGMA-%Dis (**A** and **B**), MetO (measured by HRMS with reference

calibration; **A** and **C**) and MPO (measured by ELISA; **B** and **C**). The correlation results (rho estimate, $\boldsymbol{\rho}$, and p-value) are inset for each scatterplot. CFSPID patients, identified by newborn screening with later inconclusive diagnosis of disease, are shown in red.

Figure 3. Methionine oxidation, airway MPO and neutrophils are strong correlates of bronchiectasis in early CF. We tested the Spearman correlations of PRAGMA-%Dis and PRAGMA-%Bx with BALF measures (MetO, % OxMet, MPO, total protein), BAL cell populations [percentages of neutrophils (PMNs), macrophages (MΦ), lymphocytes (Lymphs) and eosinophils (Eos)], patient age (months), patient sweat chloride (mM) and the total number of antibiotic courses received by patients in the prior 12 months. **(A)** Blue-to-red heatmap of Spearman's ρ for the indicated variables. Red = positive correlation, blue = negative correlation. The intensity of the color indicates the strength of the relationship. **(B)** Matching single-gradient white-to-red heatmap of p-values (expressed as –log(*P*)). Intensity of the red color indicates greater statistical significance. Black cells indicate results of $p > 0.05$ for the relevant pairwise correlation. Cells denoted by (X) indicate where rows and columns for the same variable meet.

Figure 4. Roles of myeloperoxidase and methionine sulfoxide in the development of early CF bronchiectasis. Neutrophil (PMN) recruitment to airways may occur in early CF without an obvious pathogenic stimulus. In the current study, methionine sulfoxide (MetO) in early CF BALF was correlated strongly with CT scores of bronchiectasis. Following influx of neutrophils that secrete myeloperoxidase (MPO) into the lumen, oxidizing activity of MPO may generate MetO from methionine. MPO

generates hypochlorous and hypobromous acid, which cause rapid, frequently irreversible damage to an array of biomolecules including tissue macromolecules. The oxidizing activity of MPO provides a common link between MetO and tissue injury which may lead to bronchiectasis. These processes may be insufficiently resolved in early CF and contribute to a feed-forward mechanism underlying sustained PMN recruitment. Whether MetO may directly participate in the promotion of CF airway disease is unclear at this time.

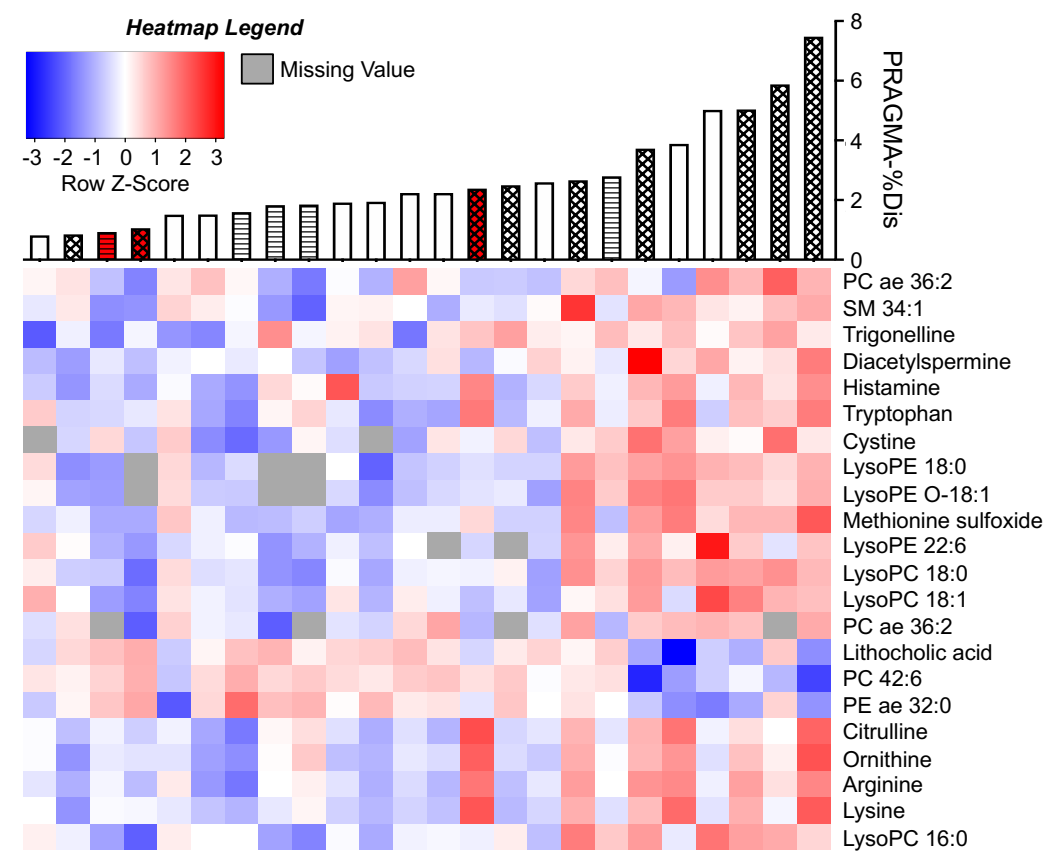
Heatmap Legend
Missing Value
-3 -2 -1 0 1 2 3
Row Z-Score
PRAGMA-%Dis
0
2
4
6
8
PC ae 36:2
SM 34:1
Trigonelline
Diacetylspermine
Histamine
Tryptophan
Cystine
LysoPE 18:0
LysoPE O-18:1
Methionine sulfoxide
LysoPE 22:6
LysoPC 18:0
LysoPC 18:1
PC ae 36:2
Lithocholic acid
PC 42:6
PE ae 32:0
Citrulline
Ornithine
Arginine
Lysine
LysoPC 16:0

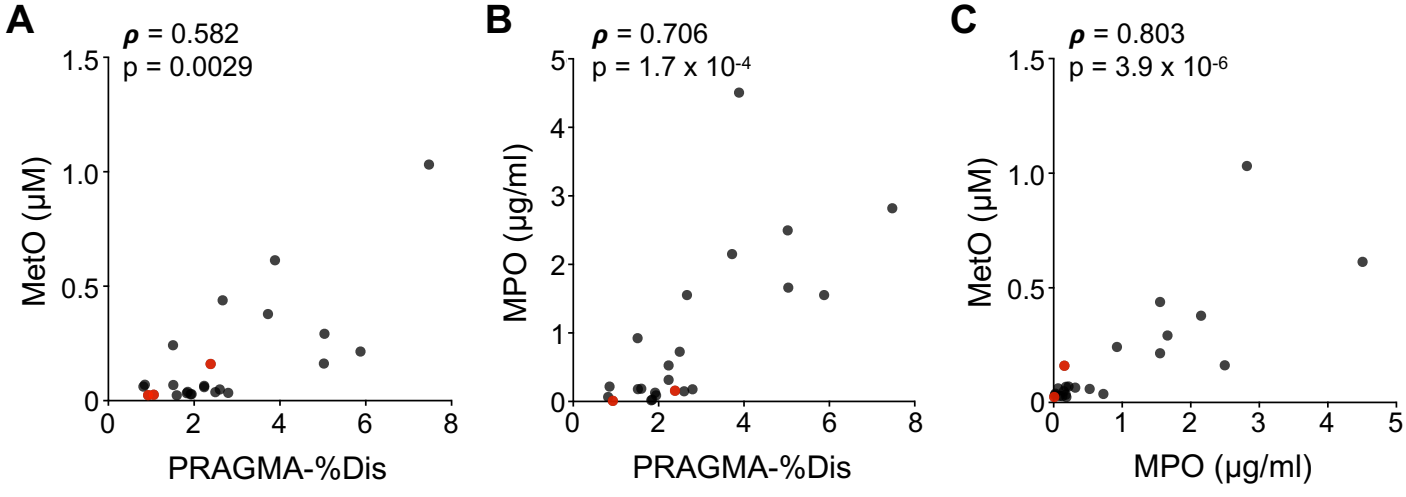
A
ρ = 0.582
p = 0.0029
MetO (µM)
PRAGMA-%Dis
B
ρ = 0.706
p = 1.7 x 10-4
MPO (µg/ml)
PRAGMA-%Dis
C
ρ = 0.803
p = 3.9 x 10-6
MetO (µM)
MPO (µg/ml)

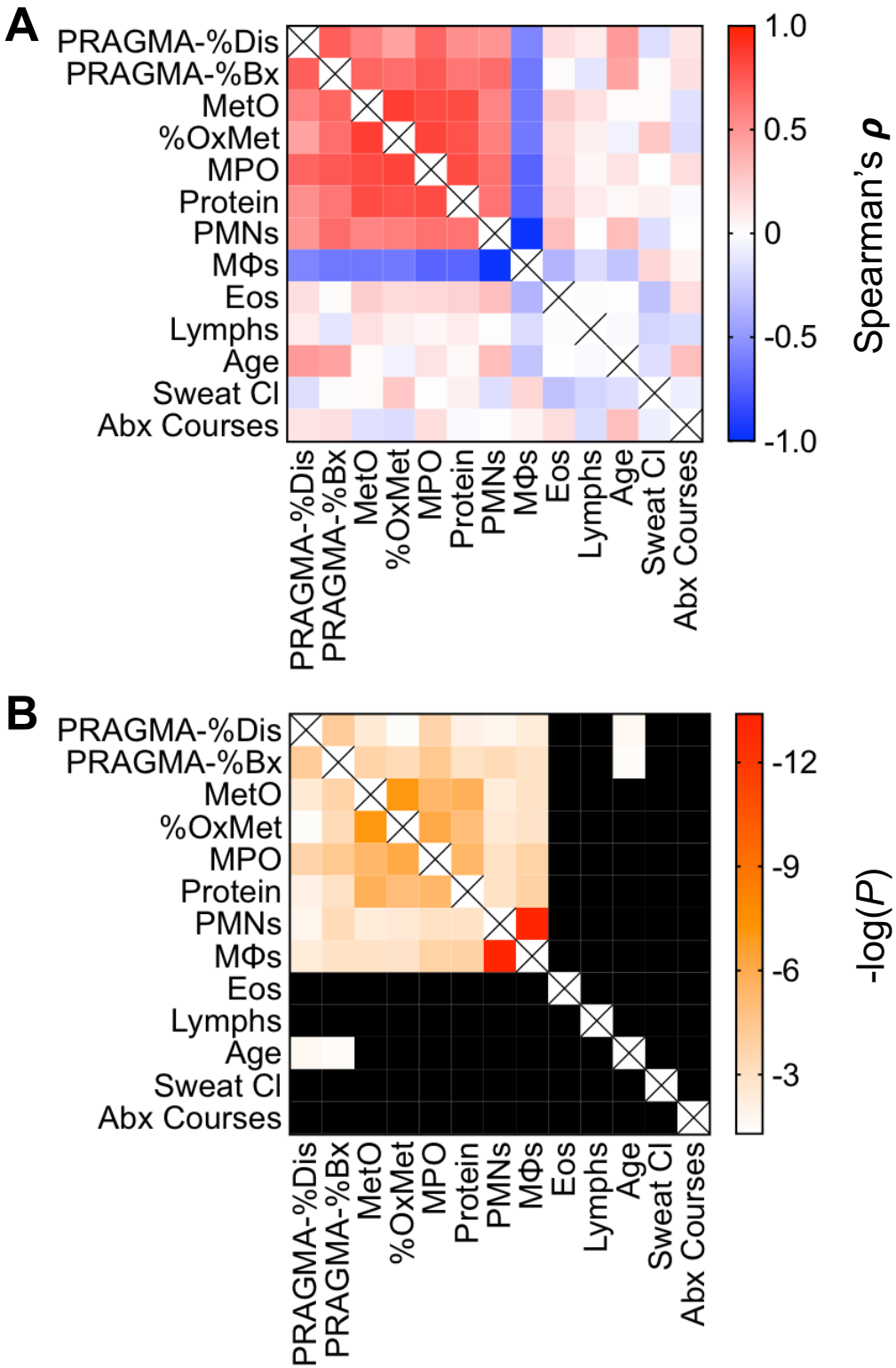
A
PRAGMA-%Dis
PRAGMA-%Bx
MetO
%OxMet
MPO
Protein
PMNs
MΦs
Eos
Lymphs
Age
Sweat Cl
Abx Courses
1.0
0.5
0
-0.5
-1.0
Spearman's ρ
B
-12
-9
-6
-3
-log(P)

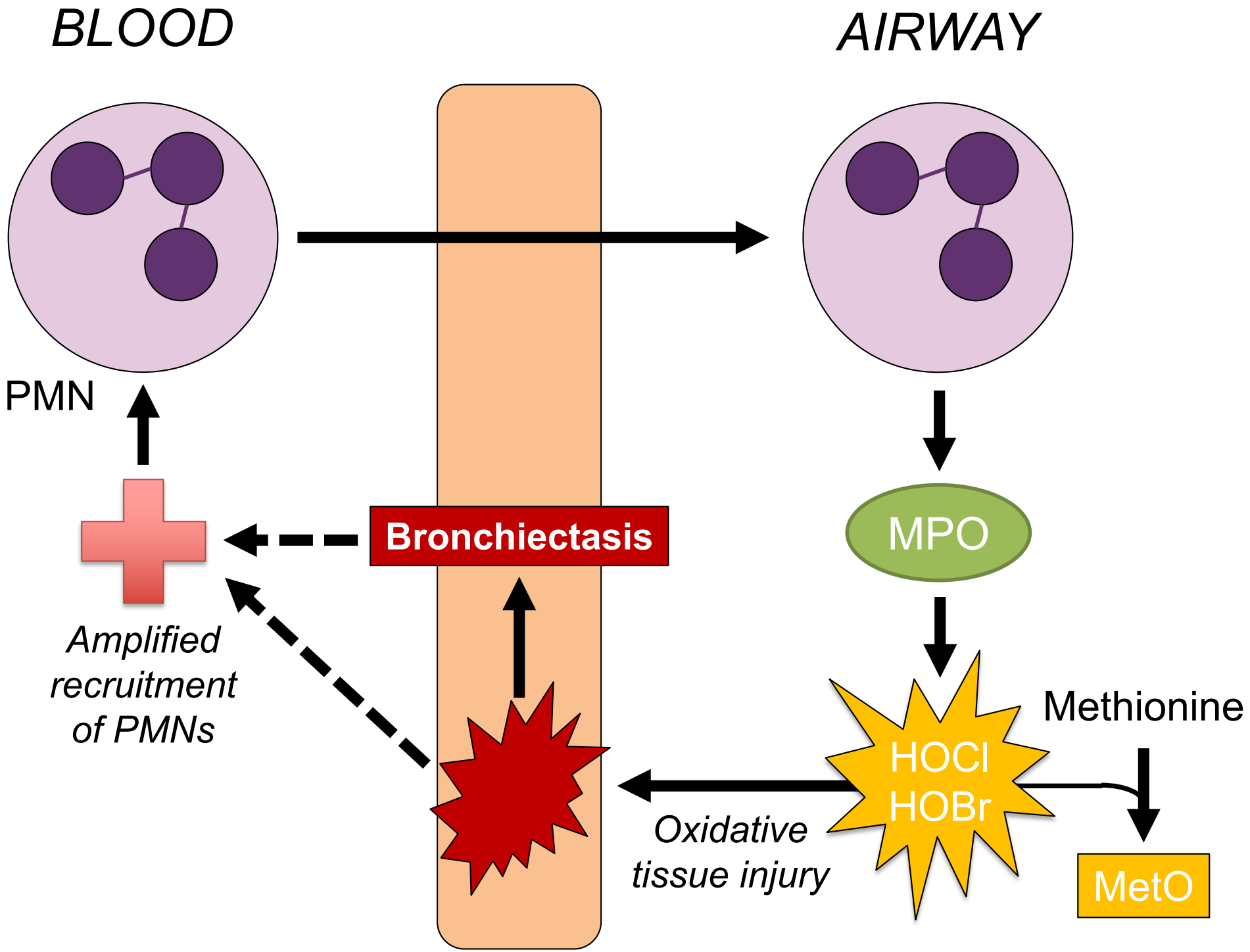
BLOOD
AIRWAY
PMN
Bronchiectasis
MPO
Amplified recruitment of PMNs
Methionine
HOCl
HOBr
Oxidative tissue injury
MetO

SUPPLEMENTARY INFORMATION

- **List of Supplementary Data Files** (with description of contents)
- **Supplementary Methods**
- **Supplementary Figures 1-5**

LIST OF SUPPLEMENTARY DATA FILES

File accession: Listed data files have been uploaded to the Dryad Digital Repository (datadryad.org) under digital object identifier (DOI) doi:10.5061/dryad.55m2m81. For direct access, use the following link: https://doi.org/10.5061/dryad.55m2m81

SFile1_RawFeatureTable.xlsx: This is a table of the raw apLCMS-based peak intensity extraction of HRMS results, including blank (Water) and quality control (NIST, QSTD) samples. Total features detected, 11,188. “NIST” refers to the SRM 1950 reference standard. “QSTD” refers to an in-house prepared mixture of human plasma. All samples were injected in triplicate and the results have been median summarized from the triplicates. The first two columns pertain to the detected *m/z* value at a specific retention time, given in seconds. The remaining columns pertain to blanks, reference standards and samples. These columns are ordered left-to-right in the order of injection. For the samples, “_A” or “_B” designations pertain to shipment batches that took place between Erasmus and Emory. Three samples were ultimately excluded from analysis: one, 25, because of aberrant global sample composition, and two others, 09_A and 15_A, because aliquots were accidentally shipped and processed two independent times

because the samples were blinded. For subsequent analyses, we arbitrarily kept 09_B and 15_B samples from the second batch and discarded their "_A" counterparts, as the "_B" versions were believed to have undergone fewer freeze-thaw cycles than "_A" samples.

SFile2_HRMSResults.xlsx: This is the results file of the untargeted analysis using an in-house R package (https://github.com/kuppal2/xmsPANDA) on raw HRMS data after removing features that did not meet data quality thresholds and dropping poor quality and redundant samples. QC materials were not analyzed in the untargeted test. Columns A-B pertain to observed *m/z* and retention time. Columns C-E pertain to accurate mass matches to the features (Annotation, Adduct, and ppm mass accuracy error; see Supplementary Methods for details). After accurate mass matching, spectral convolutions (i.e., isotopes and neutral losses) were designated by manual inspection of co-elution, intensity correlation and *m/z* shift. Retention times were taken into consideration for assignments (e.g., longer retention times generally correspond to hydrophilicity and spectral convolutions of adducts and isotopes should co-elute). Note, the [M+H] ion of lidocaine (235.1804 *m/z* by 127.6 sec; used as local anesthetic during bronchoscopy) held the maximum intensity value in each sample and was normalized to the same maximal value in each distribution, resulting in its removal during testing. Ppm error was calculated by METLIN except for spectral convolutions, which were calculated manually. Accurate mass annotations are only provided for those results that met significance criteria ($p < 0.05$, $q < 0.25$). Columns F-H indicate the raw p-value ("P.value"), q-value ("adjusted.p.value") and Pearson's *r* statistic ("Estimate_var1"),

respectively. Remaining columns show log_2-transformed and quantile normalized HRMS intensities for each of the study samples. Missing values were imputed as “NA” to avoid skewing the correlation. The sample columns were automatically ordered from low-to-high PRAGMA-%Dis.

SFile3_ClinicalData.xlsx: These data correspond to important clinical variables for the patient samples analyzed in this study.

SFile4_FollowUpStudiesData.xlsx: Results used for follow-up studies with Spearman’s correlations. MetO and methionine (Met) quantifications are based on reference calibration relative to the concentrations determined for SRM 1950 reference material. MPO measurements are based on the ELISA assay.

SUPPLEMENTARY METHODS

Metabolomics

Metabolites were extracted from BALF by 1:2 mixture with acetonitrile (ACN) plus a mixture of internal standards. Internal standards from Cambridge Isotope Labs were added to all samples at the following final concentrations: [$^{13}C_6$]-D-glucose (5 mM), [^{15}N]-indole (10 µM), [$^{13}C_5$,^{15}N]-L-methionine (25 µM), [2-^{15}N]-L-lysine dihydrochloride (150 µM), [^{15}N]-choline chloride (8 µM), [$^{13}C_5$]-L-glutamic acid (25 µM), [$^{13}C_7$]-benzoic acid (10 µM), [^{15}N]-L-tyrosine (50 µM), [$^{15}N_2$]-uracil (0.1 µM), [3,3-$^{13}C_2$]-cystine (60 µM), and [trimethyl-$^{13}C_3$]-caffeine (10 µM). The extract supernatant was isolated after centrifugation at 16,100 *g* x 10 min at 4 ˚C and transferred to autosampler vials. Reference standards extracted and analyzed in parallel were National Institute of Standards and Technology (NIST) standard reference material (SRM) 1950 plasma and a separate pooled plasma sample prepared for batch QC purposes. Vials of extract supernatant were maintained at 4 ˚C on the autosampler tray while awaiting injection. Ten µl of supernatant were injected into an Accucore HILIC 100 x 2.1 mm column (2.6 µm particle size, 80 Å pore size) with a 10 x 2.1 mm matching pre-column, held at 30 ˚C with mobile phases of 100% water, 100% ACN and 2% aqueous formic acid. Starting conditions were 20% water/80% ACN held for 1.5 min at a flow rate of 350 µl/min, followed by a linear gradient to 90% water/10% ACN over 4.5 min and a simultaneous flow rate gradient to 500 µl/min. These conditions were held for 9 min prior to 5 min of re-equilibration at 20% water/80% ACN. Formic acid was maintained at 0.2% throughout. Column eluate was introduced to a HESI source held at +2.5 kV. Thermo Q Exactive High Field quadrupole scanning was set at 85-1275 *m/z* and Orbitrap

resolution was set to 120,000 full width at half maximum. After feature alignment by apLCMS and data quality assessment by xMSanalyzer, a list of 11,188 *m/z*-by-retention time features was extracted. These were further selected for analysis based on thresholds for mean sample intensity ($<10^6$), mean sample intensity relative to water blanks (<1.5-fold that of water), missing values (>20% among samples), median technical replicate coefficient of variation (>20%) and retention time (<30 seconds, corresponding to void volume). Two redundant samples and one with aberrant missing values were dropped (see '*SFile1_RawFeatureTable.xlsx*'). The final list contained 1,798 *m/z*-by-retention time features for analysis. After completion of Pearson's correlation of each feature with PRAGMA-%Dis (see '*SFile2_HRMSResults.xlsx*'), significant ($p<0.05$, $q<0.25$) features were annotated using METLIN (metlin.scripps.edu) with a ppm ≤ 3 mass accuracy threshold and searching for [M+H], [M+Na], [M+H-H2O], [M+K], [M+2H] and [M+2Na-H] adducts. Reference calibration of BALF samples by SRM 1950 to estimate absolute concentrations of MetO and Met was carried out by multiplying the ratio of sample intensities to the average SRM 1950 intensity by the observed concentrations in SRM 1950. I.e., $(\text{Intensity}_{\text{sample}}/\text{mean Intensity}_{\text{SRM 1950}})*(C_{\text{SRM 1950}})$.

For validation and quantification of methionine sulfoxide (MetO), an isotopically enriched standard of $^{13}C_5$,^{15}N-L-MetO and $^{13}C_5$,^{15}N-L-methionine (Met) was made by adding sodium hypochlorite dropwise to $^{13}C_5$,^{15}N-L-Met in PBS pH 7.4 to a final ratio of 1:10. Resulting $^{13}C_5$,^{15}N-L-MetO and $^{13}C_5$,^{15}N-L-Met were measured as 0.294 and 1.613 mM (respectively) by calibrating with pure reference standards (Sigma-Aldrich). The

heavy-labeled standard was used to confirm co-elution and MS/MS in SRM 1950 and pooled BALF, and to quantify the compounds in SRM 1950 for reference calibration.

Heatmaps and chromatograms were visualized using R 3.3.3 (www.R-project.org) and chemical structures were generated in ChemDraw 16.0 (Perkin Elmer).

MPO Assay

Samples were assayed at dilutions of 200-, 100- and 20-fold. Unless stated otherwise, dilutions were in assay buffer containing 1% bovine serum albumin and 0.025% Tween-20 in phosphate-buffered saline, pH 7.4 (PBS); wash steps were 3 x 10 minutes of 200 µl PBS with 0.05% Tween-20; reaction volumes were 50 µl; and temperature ambient. First, monoclonal rabbit anti-MPO (Abcam ab10165) diluted 1:800 in PBS was plated overnight on black, clear-bottomed high-binding microtiter plates (Greiner). Wells were blocked with 75 µl assay buffer for 2 hours prior to washing and addition of MPO standard (EMD) or samples for 1 hour at 37 ˚C. Wells were washed and activity was measured by the addition of 50 µM Amplex Red (Invitrogen), 20 µM hydrogen peroxide and 50 mM sodium bromide in 50 mM sodium phosphate buffer, pH 7.4 with final 0.1% DMSO. Fluorescence was measured at $544_{Ex}/590_{Em}$ at 3, 6, 9 and 12 minutes on SpectraMax iD3 instrumentation (medium photomultiplier tube gain, 1.0 mm read height from top). Wells were washed, probed with 1:500 polyclonal rabbit anti-MPO (Abcam ab9535) at 37 ˚C for 1 hour, washed again, probed with 1:5000 biotin-conjugated goat anti-rabbit IgG (Agilent-Dako E034201-6) for 1 hour with assay buffer containing 0.05% Tween-20, washed again, incubated with 1:1000 ExtrAvidin-alkaline phosphatase (Sigma) for 1 hour, washed a final time and developed with 1-Step para-

nitrophenyl phosphate solution (ThermoFisher). Absorbance at 405 nm was measured at 10, 20, 30 and 40 minutes. Four-parameter logistic (4PL) curve fits were used for sample calibration. For samples quantifiable within multiple dilutions, the result assayed closest to its 4PL inflection point was selected.

MPO Western blot

Protein from pooled BALF, lysed human neutrophils from two healthy adults and human MPO standard (EMD) were reduced with 50 mM beta-mercaptoethanol at 80 ˚C for 15 minutes in 1X final concentration of Laemmli buffer (Bio-Rad). We then loaded 1.7 µg of protein or 1-100 ng of pure MPO per well on a 15-well 4-20% Mini-PROTEAN TGX gel (Bio-Rad). Proteins were transferred to a polyvinylidene difluoride membrane using a Trans-Blot turbo set to 'Mixed' size range optimization. MPO was developed using 1:1,000 polyclonal rabbit anti-MPO (Abcam ab9535) followed by 1:10,000 goat anti-rabbit-conjugated IRDye 680RD (Li-Cor 925-68071). The membrane was imaged using a 3.0 intensity level.

Total protein measurement

Neat CF BALF was assayed to measure total soluble protein in triplicate using the BCA Protein Assay Kit (Pierce). Bovine serum albumin diluted in 0.9% saline with 0.05% NaN_3 (Pierce) was used as the reference standard from 31.25 to 2,000 µg/ml.

SUPPLEMENTARY FIGURES

Supplementary Figure 1. Analyses of global variation and data distribution. (A) Analytical features from HRMS analysis of 25 CF BALF samples were loaded in MetaboAnalyst (http://www.metaboanalyst.ca/) for principal components analysis. Sample 25 was an outlier, separating from other BALF samples on PC1 and PC2. Also note the anticipated separation of BALF and plasma reference samples (SRM 1950, in-house QSTD), and their respective clustering. Two separately shipped batches of BALF from Erasmus to Emory ('BAL1', 'BAL2') were also evaluated for possible signs of cluster separation (not observed). **(B)** Counts of missing values of HRMS analysis in all BALF samples. Sample 25 has >20-fold more missing values than the median of all samples. We concluded that Sample 25 should not be analyzed. **(C)** After removing Sample 25 and QC samples, the post-transformation distribution of metabolites in BALF was visualized to confirm the appropriateness of untargeted Pearson correlation analysis.

Supplementary Figure 2. Confirmation of accurate mass match to methionine sulfoxide. 166.0533 *m/z* at 4.7 min retention time was detected in BALF and SRM 1950 reference material and matched to the [M+H] adduct of methionine sulfoxide (MetO). **(A)** Full scan ion chromatrogram of naturally occurring MetO. Trace is the average of three technical replicates of a representative CF BALF sample. **(B)** 30% HCD MS/MS spectra of naturally occurring MetO in pooled CF BALF. Five peaks of decreasing *m/z* corresponding to the expected fragmentation of MetO are shown in red, as well as the molecular ion. Unassigned spectra are depicted in blue. Respective observed peak *m/z* values at maximum recorded intensity are as follows (formula assignments in

parentheses): [M+H], 166.0535 ($[C_5H_{11}NO_3S+H]^+$); 1, 149.0264 ($C_5H_9O_3S$); 2, 102.0552 ($C_4H_8NO_2$); 3, 75.0267 (C_3H_7S); 4, 74.0240 ($C_2H_4NO_2$); 5, 56.0499 (C_3H_6N). The unassigned base peak (denoted by *) is cut off at 20% intensity for better visualization. **(C)** Relative intensities of MetO-assigned MS/MS spectra (1-5 and [M+H]) in pooled BALF and SRM 1950 plasma. Spectra of $^{13}C_5$,^{15}N-L-MetO internal standard (Istd) in both matrices were also analyzed and included. Istd peaks were shifted by three to six amu, depending on the reaction. **(D)** Structural assignment of L-MetO to 166.0532 *m/z* based on accurate mass and retention time matches and MS/MS fragmentation. Reactions corresponding to peaks 1-4 are shown. Peak 5, which requires two neutral losses, is not depicted. Note, the two chiral centers (corresponding to the D/L alpha carbon and the R/S oxo-sulfur) were not resolved. The identity is assumed to be predominantly L-MetO according to mammalian biological norms.

Supplementary Figure 3. Comparative Western blot of BALF and blood neutrophil MPO. 1.7 µg of total protein or the indicated amounts of pure hMPO standard (EMD Millipore) were loaded into 15 µl wells after reducing with beta-mercaptoethanol, separated by SDS-PAGE (4-20% gel) and transferred to a PVDF membrane using a Trans-Blot Turbo (Bio-Rad). MPO was developed using the ELISA primary (1:1,000) and IRDye 680RD goat anti-rabbit (1:10,000; Li-Cor) at 3.0 intensity (700 nm filter; Li-Cor Odyssey Imager). Three known bands (59, 39, 13.5 kDa) and an additional band (23 kDa) were observed. Pooled early CF BALF, “B2+3”; blood neutrophils from healthy donors, “B.PMNs1” and “B.PMNs2”.

Supplementary Figure 4. Specific activity of myeloperoxidase in early CF BALF. **(A)** Normalization of MPO data with BALF total protein produces a similar distribution to that of volume-normalized results (both are non-normal). Because BALF protein is confounded by the inflammatory exudate, we opted not to use protein-normalized data. **(B)** Significant difference in intra-sample quantification by Wilcoxon matched-pairs signed rank test. The mean difference of the two methods was 0.54 µg/ml (Amplex Red – ELISA). * indicates $p < 0.05$. **(C)** Quantification of MPO by the Amplex Red method was divided by the ELISA results and multiplied by 100 to produce the estimated active percentage of MPO. Mean, 133±52%. CFSPID samples are indicated in red.

Supplementary Figure 5. Subset analysis of MetO, MPO and PRAGMA-CF correlations. Samples with >4 weeks between CT and BAL procedures and those designated as CFSPID were removed from the analysis to determine if observed correlations were robust. Spearman correlations were analyzed for MetO with PRAGMA-%Dis (A), PRAGMA-%Bx (B) and MPO (C). Correlations were also analyzed for MPO with PRAGMA-%Dis (D) and PRAGMA-%Bx (E). The correlation results (rho estimate, ρ, and p-value) are inset for each scatterplot.

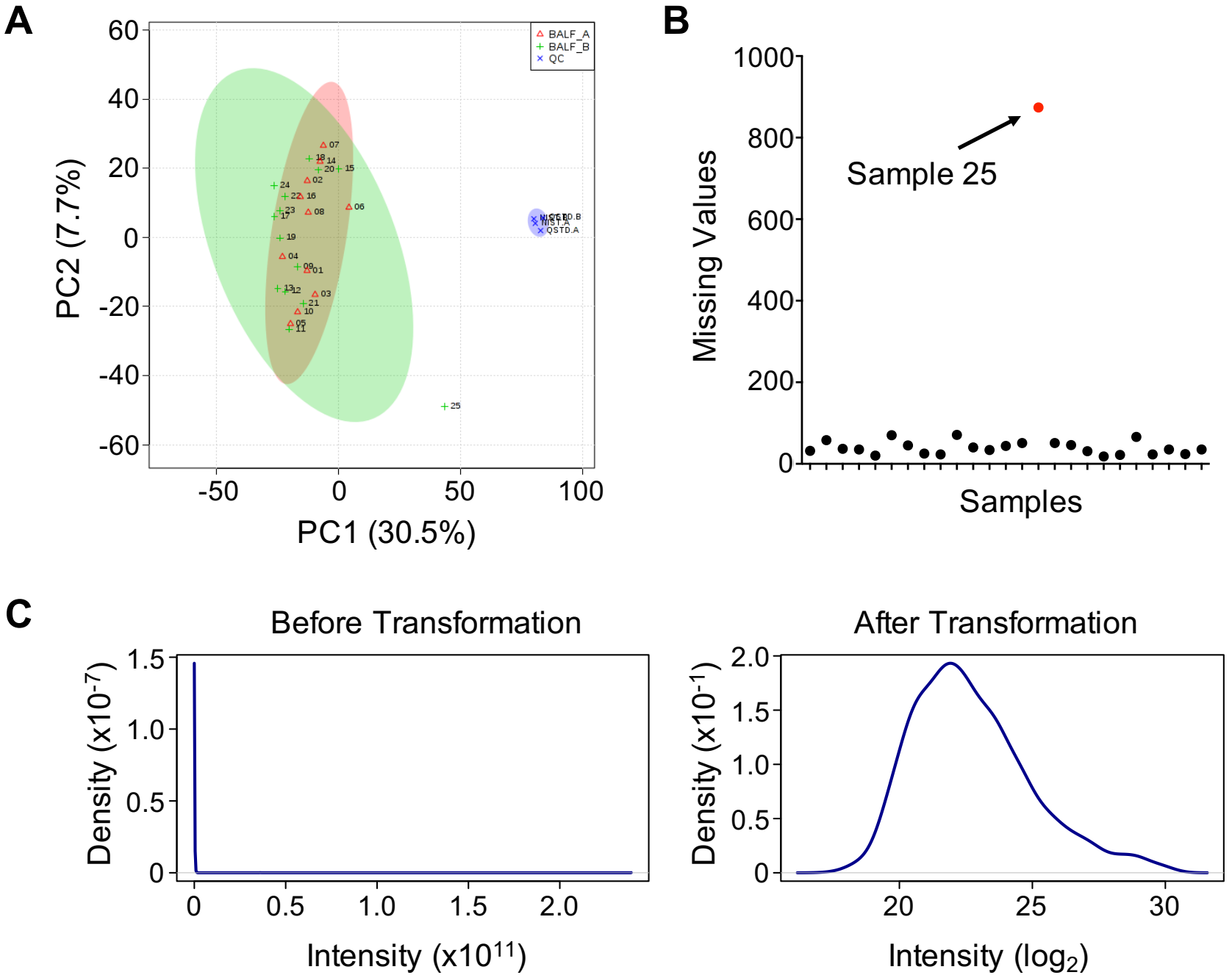
A
BALF_A
BALF_B
QC
PC2 (7.7%)
PC1 (30.5%)
B
Missing Values
Sample 25
Samples
C
Before Transformation
Density (x10-7)
Intensity (x1011)
After Transformation
Density (x10-1)
Intensity (log2)

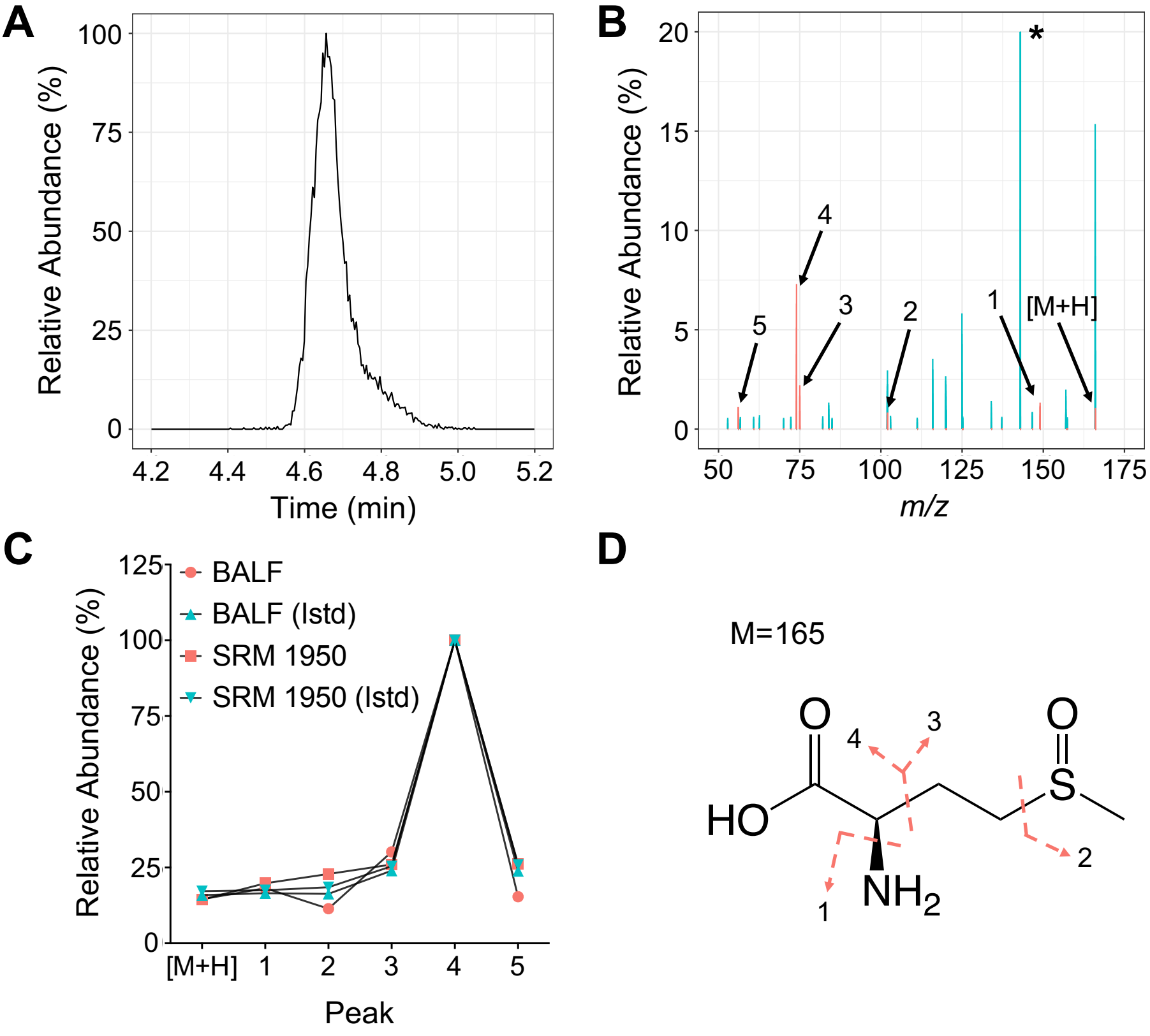
A
Relative Abundance (%)
100
75
50
25
0
4.2
4.4
4.6
4.8
5.0
5.2
Time (min)
B
Relative Abundance (%)
20
15
10
5
0
*
4
3
5
2
1
[M+H]
50
75
100
125
150
175
m/z
C
Relative Abundance (%)
125
100
75
50
25
0
BALF
BALF (Istd)
SRM 1950
SRM 1950 (Istd)
[M+H]
1
2
3
4
5
Peak
D
M=165
O
HO
4
3
O
S
2
1
NH2

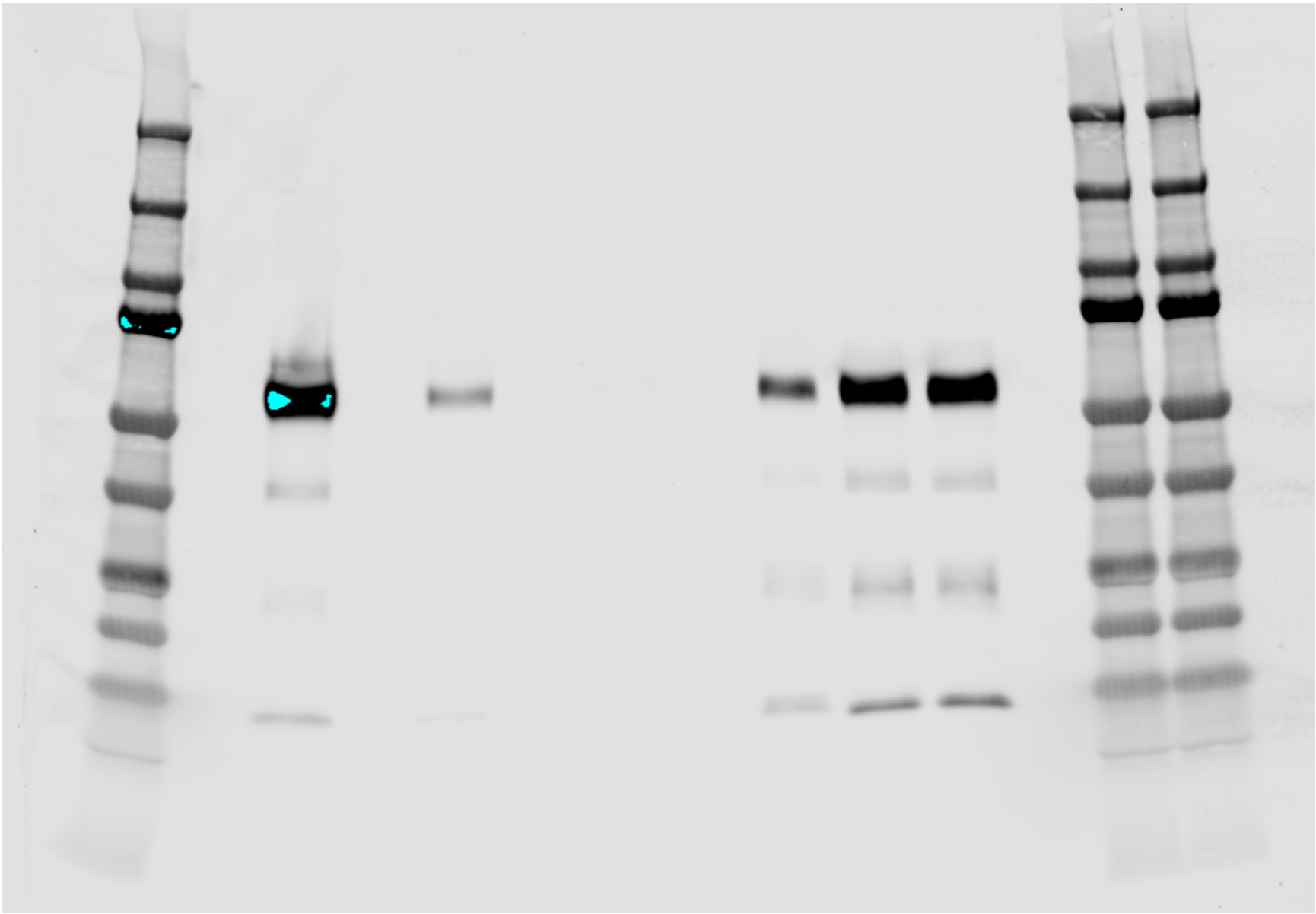
250
150
100
75
50
37
25
20
15
10
100 ng
10 ng
1 ng
B2+3
B.PMNs1
B.PMNs2

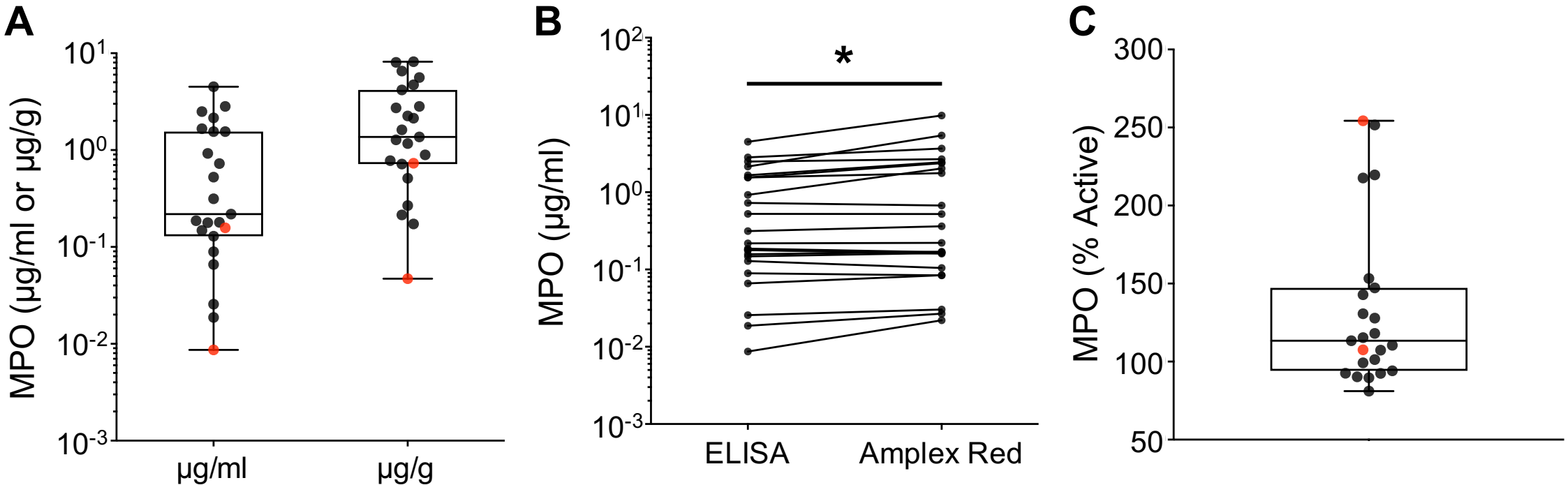
A
MPO (µg/ml or µg/g)
10^1
10^0
10^-1
10^-2
10^-3
µg/ml
µg/g
B
MPO (µg/ml)
10^2
10^1
10^0
10^-1
10^-2
10^-3
*
ELISA
Amplex Red
C
MPO (% Active)
300
250
200
150
100
50

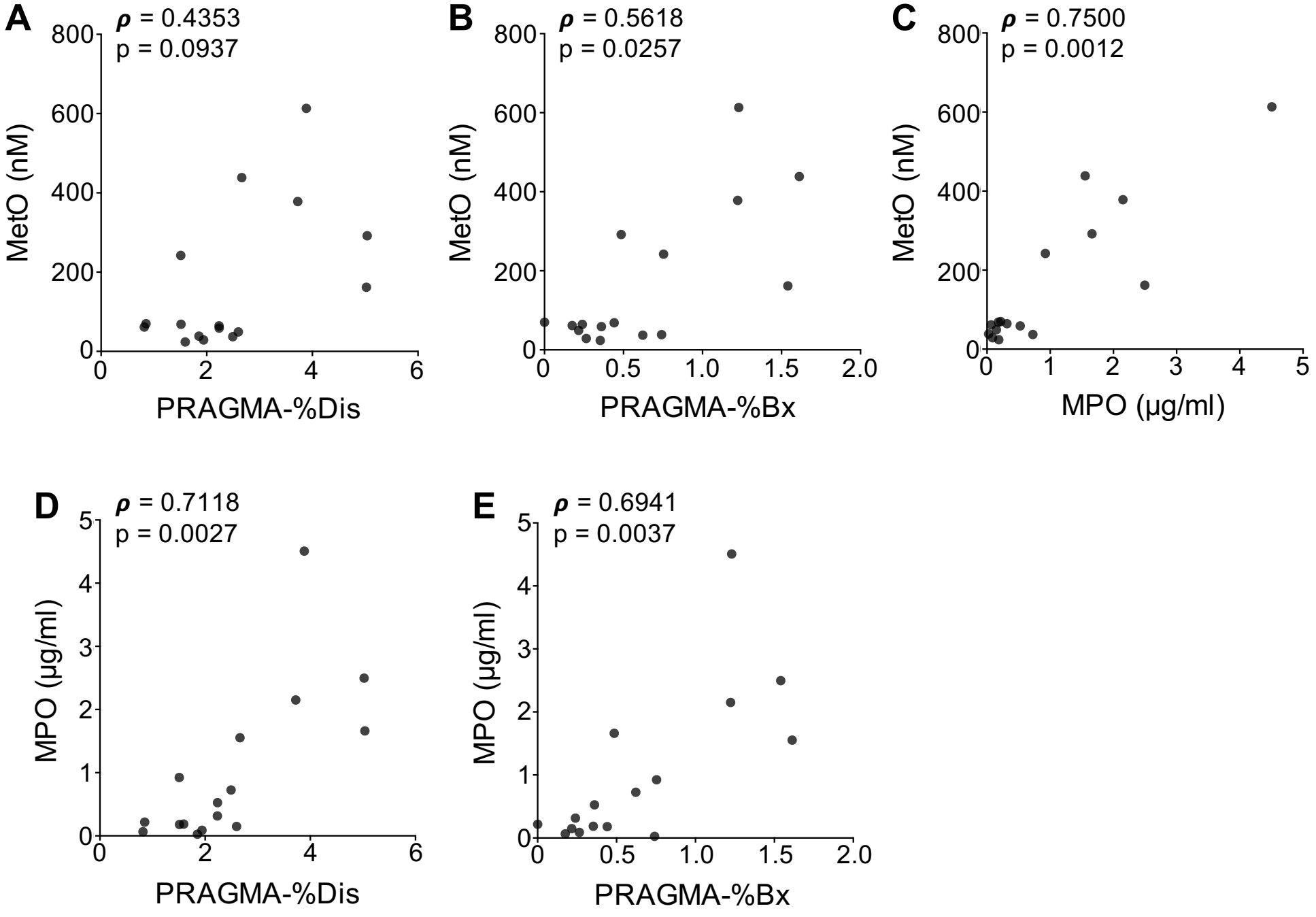
A
ρ = 0.4353
p = 0.0937
MetO (nM)
PRAGMA-%Dis
B
ρ = 0.5618
p = 0.0257
MetO (nM)
PRAGMA-%Bx
C
ρ = 0.7500
p = 0.0012
MetO (nM)
MPO (µg/ml)
D
ρ = 0.7118
p = 0.0027
MPO (µg/ml)
PRAGMA-%Dis
E
ρ = 0.6941
p = 0.0037
MPO (µg/ml)
PRAGMA-%Bx